Flat surface measurements on fiber point diffraction interferometer

Lingfeng Chen, Yaqing Ren, and Jie Li
Beijing Institute of Technology, School of Optoelectronics, Beijing, 100081 China
E-mail: djkclf@bit.edu.cn

Abstract. We present a two-step program for point-by-point flat surface measurements with a fiber point diffraction interferometer (FPDI). The point diffraction wavefront reflected by a flat mirror under test is an aberrated spherical wavefront carrying the surface information of the flat mirror. The aberrated spherical wavefront interferes with a reference point diffraction wavefront through a plate beamsplitter (BS). The aberrations of the plate BS are also measured by the FPDI method. The figure of the flat mirror can be evaluated point by point after correcting the aberrations of the plate BS. This method makes use of the nearly perfect point diffraction wavefront, thus it can assure accurate flatness measurement on the optic under test. This research extends to the field of FPDI applications, and provides a new route for the high precision measurement of flat optics. © *2010 Society of Photo-Optical Instrumentation Engineers.*
[DOI: 10.1117/1.3432575]

Subject terms: interferometers; diffraction; optical testing.

Paper 100106LR received Feb. 9, 2010; revised manuscript received Apr. 1, 2010; accepted for publication Apr. 26, 2010; published online May 28, 2010.

1 Introduction

There is a long history of absolute testing techniques for flat surfaces. Liquid surfaces have been used as a natural reference flat, but problems with vibrations, dust, the meniscus region near the walls of the vessel, and the curvature of the earth all limit the accuracy of such a measurement.[1] The well-known "three flat test" devised by Schulz and Schwider[2] has been used for decades, but this test only gives an absolute point-by-point measurement along one diameter of a flat. Extensions from single lines to 2-D absolute deviation values have extensively been discussed in several publications.[3–6]

This work follows the idea of finding a more ideal reference wavefront to make an absolute point-by-point flatness measurement over an area. The point diffraction interferometer (PDI) invented by Smartt and Strong has very high accuracy because it employs a nearly ideal spherical wavefront diffracted by a small aperture.[7] Almost all the early PDIs generated the ideal wavefront with the pinhole method. As fiber fabrication technology advanced, optical fibers with a core diameter of only several microns became capable of serving as good point diffraction sources that provide a high quality reference wave. FPDI has been applied in the optical testing of off-axis aspheric mirrors,[8] spherical mirrors,[9] and converging optics.[10]

Due to the diverging characteristic of the point diffraction wavefront, a PDI cannot be directly used in a flat surface measurement. Utilizing the high precision point diffraction wavefront in a flat surface measurement is valuable research in practice.

2 Flat Surface Measurement on Fiber Point Diffraction Interferometer

The point diffraction wavefront reflected by a flat mirror is an aberrated spherical wavefront carrying the surface information of the flat mirror. By letting this aberrated spherical wavefront interfere with a reference point diffraction wavefront, we can measure the wavefront aberrations of the flat mirror. This can be done through introducing a plate beamsplitter (BS). However, the plate BS also introduces errors into the measurement. If we can eliminate its wave aberrations from the measurement results, then the flat surface can be retrieved.

2.1 *Step 1*

In Fig. 1, the optic under test is a flat mirror. The beam from a laser source passes through a variable neutral density filter and a half-wave plate, and is split into two orthogonally polarized beams by a polarization prism BS. One beam is reflected from a retroreflector mounted on a piezoelectric phase shifter, and the other beam is reflected from a retroreflector mounted on a variable delay line. Both beams pass twice through quarter-wave plates to rotate their polarizations. After passing through polarizers, they are coupled into fiber 1 and fiber 2 separately. The relative intensity between the two beams can be adjusted by the angular orientation of the half-wave plate and the polarizers.

The spherical wavefront diffracting from fiber 1 is reflected by the flat mirror under test, and redirected to the plate BS. The reflected wavefront is still a spherical wavefront that contains aberrations of the flat mirror; its sphere center is in the virtual image point P at the end of fiber 1 in the flat mirror. It becomes the measurement wavefront after passing through the plate BS. The end of fiber 2 is placed at the point P′, which is conjugate to point P with respect to the plate BS. The spherical wavefront diffracting from fiber 2 is reflected by the plate BS (reference wavefront) and interferes with the measurement wavefront.

The interference patterns are imaged onto a charge-coupled device (CCD) camera through a relay lens. The wavefront abrrations are analyzed using standard phase extraction algorithms. This step measures the aberrations of the flat mirror as well as those of the plate BS.

2.2 *Step 2*

In Fig. 2, fiber 2, the plate BS, CCD camera, imaging lens, relay lens, and other optics are all kept in exactly the same positions. It is important that they are not moved between the two measurements. The flat mirror under test is removed, and the end of fiber 1 is placed at point P. The measurement wavefront diffracting from fiber 1 passes through the plate BS and interferes with the reference wavefront diffracting from fiber 2. This measurement can evaluate the aberrations introduced by the plate BS.

To obtain the aberrations due to just the flat mirror, the result of the second measurement is subtracted from the result of the first measurement. Because the optical path remains the same during these two measurements, the sub-

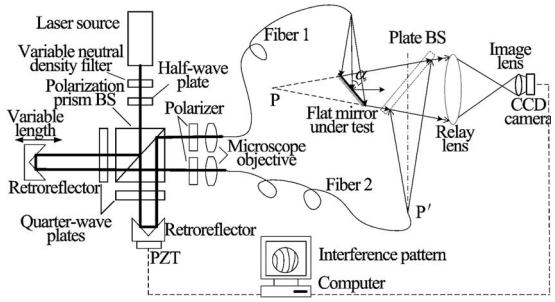

Fig. 1 The flat surface measurement on the FPDI (step 1).

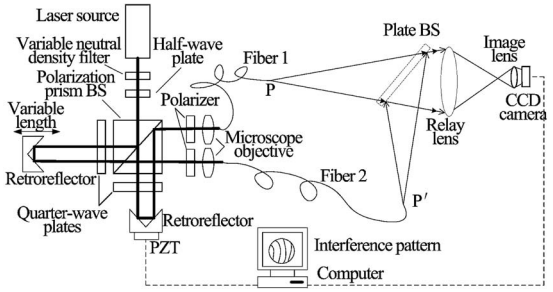

Fig. 2 The flat surface measurement on the FPDI (step 2).

traction will automatically eliminate all the aberrations introduced by the relay lens and the imaging lens at the same time. However, the incident wave to the flat mirror is not a plane but spherical; its incident angle varies from point to point at the mirror surface. Supposing $w(i,j)$ is the calculated wave aberration at coordinate (i,j) of the flat mirror, the surface figure $s(i,j)$ of the flat mirror is related to the aberration $w(i,j)$ by,

$$s(i,j) = w(i,j) \cdot \cos[\alpha(i,j)]/2 = k_{i,j} \cdot w(i,j), \quad (1)$$

where $k_{i,j}=\cos[\alpha(i,j)]/2$, $\alpha(i,j)$ is the incident angle at coordinate (i,j) of the flat mirror (see Fig. 1), and $k_{i,j}$ is the correcting factor at coordinate (i,j).

3 Experimental Results

We use a circular flat mirror with a diameter of 25 mm to verify the program. The plate BS is 145 mm in length, 85 mm in breadth, and 19 mm in thickness. The wavelength of the laser source is 532 nm. The core diameter of the single mode fiber is 3.5 μm, and its numerical aperture is 0.13. The deviation of the fiber's diffracting wavefront from a true sphere is demonstrated to be less than $\lambda/10^4$,[8] and thus can be ignored during the measurement.

First, the flat mirror is placed near the plate BS in the light path, about 210 mm away from the end of fiber 1. To facilitate the placement and adjustment of the optics and the imaging systems, we set the incident angle as 45 deg. However, an incident angle as close as possible to normal incidence would be much more appropriate. The beam reflected by the mirror has an elliptical outline in the case of oblique incidence, but its ellipticity is not obvious because the flat mirror is placed far from the fiber. We use a circular aperture to get circular interference patterns; the aperture filters out about 5% of the mirror outside. The relative intensity between the measurement and reference beams, together with the optical path difference of the two beams, are adjusted and matched to produce interference patterns with maximum possible contrast. Because the interference comes from two point light sources, the end of fiber 2 (P′) should be placed where the interference patterns are as linear as possible to minimize the power error. Then, the flat mirror is removed. An auxiliary spherical mirror is placed behind the relay lens to reflect back the beam of fiber 2, and the converging point at the left side of the plate BS indicates the approximate position of point P. The end of fiber 1 is placed at point P to measure the wavefront aberrations of the plate BS. Figures 3(a) and 3(b) are the interference patterns obtained during the experiments. We can find apparent astigmatism aberration from Fig. 3, mainly due to the plate BS bringing aberrations into the diverging measurement beam. However, the aberrations introduced by the plate BS have nothing to do with the final results, because it can be eliminated in the subtraction afterward.

A five-step phase reconstruction algorithm is applied to process the interference patterns. The wave aberrations of the flat mirror can be retrieved by subtracting the reconstructed phase of the plate BS from the compound wavefront point by point. From ten repeated tests, the random measurement errors of the peak-to-valley (PV) profile are found to be 176.6 ± 2.7 nm, and the rms magnitude of the overall wavefront is 36.8 ± 0.5 nm. In our configurations, the incident angle from fiber 1 to the flat mirror varies between [41.5 to 48.5 deg]. To simplify the calculations in Eq. (1), we use an average correcting factor $\bar{k}_{i,j}$ to correct the wave aberrations of the flat mirror $\bar{k}_{i,j}=\cos 45\ \text{deg}/2 \approx 0.354$. After the angle corrections, the PV surface error of the flat mirror is 62.4 ± 1.0 nm, and the rms surface error is 13.0 ± 0.2 nm. Figure 4(a) shows the measured surface of the flat mirror, with piston and tilt removed.

As a comparison, the surface of the flat mirror measured by a Zygo GPI-XP interferometer (ZYGO, Middlefield, Connecticut) is also shown in Fig. 4(b). The PV surface error measured by ZYGO is 57.6 nm; the rms surface error

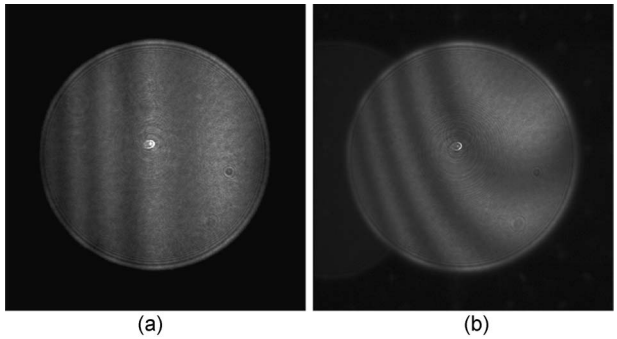

Fig. 3 Interference patterns obtained during the experiments. (a) Interference patterns captured in step 1. (b) Interference patterns captured in step 2.

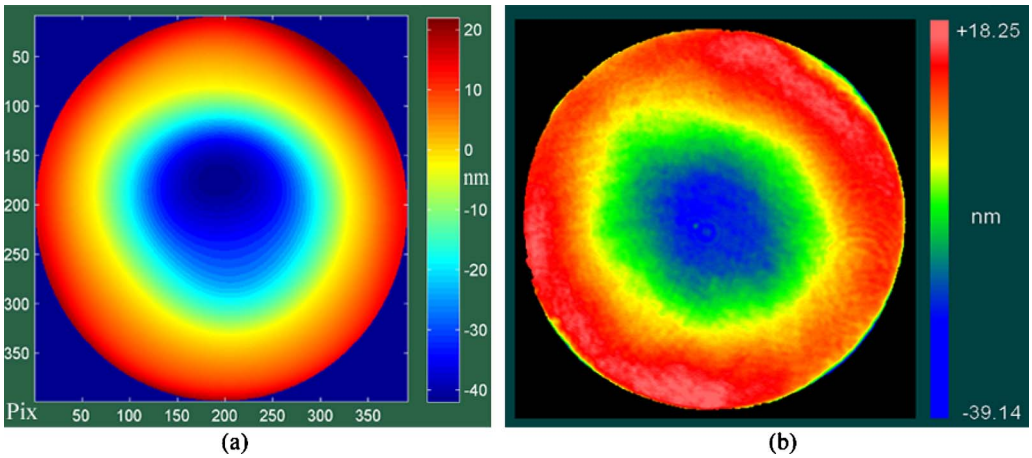

Fig. 4 Measured profile of the flat mirror, with piston and tilt removed. (a) Profile measured by the two-step method on the FPDI. (b) Profile measured by the ZYGO GPI-XP interferometer.

is 11.4 nm (the surface is also trimmed 5% of the mirror outside). We can see that its contour shape is the same with Fig. 4(a). The absolute PV difference of the two results is 4.8 nm, and the rms difference is 1.6 nm. These differences can be mostly attributed to the different reference wavefront used by these two interferometers as well as the approximations during the angle corrections. Taking measurement uncertainty into account, the two results can be regarded as consistent.

4 Conclusion

By introducing a plate BS, we present and verify a two-step flat surface measurement program on the FPDI. Since the flat surface is tested in diverging wavefronts, this method is in essence a Richey-Common test that was adapted to the peculiarities of the point diffraction interferometer. However, because this method makes use of the nearly perfect point diffraction wavefront, it can assure accurate point-by-point flatness measurement on the optic under test. This research extends the field of FPDI applications, and provides a new route for the high precision measurement of flat optics.

Acknowledgments

The work presented here is supported by the Research Fund for the Doctoral Program of Higher Education sponsored by the Ministry of Education of Chine.

References

1. D. Malacara, "Liquid reference flats," Chap.1 in *Optical Shop Testing*, D. Malacara, Ed., pp. 23, John Wiley and Sons, New York (2007).
2. G. Schulz and J. Schwider, "Precise measurement of planeness," *Appl. Opt.* **6**(6), 1077–1084 (1967).
3. B. S. Fritz, "Absolute calibration of an optical flat," *Opt. Eng.* **23**(4), 379–383 (1984).
4. U. Griesmann, "Three-flat test solutions based on simple mirror symmetry," *Appl. Opt.* **45**(23), 5856–5865 (2006).
5. M. F. Küchel, "A new approach to solve the three flat problem," *Optik (Stuttgart)* **112**, 381–391 (2001).
6. K. R. Freischlad, "Absolute interferometric testing based on reconstruction of rotational shear," *Appl. Opt.* **40**, 1637–1648 (2001).
7. R. N. Smartt and J. Strong, "Point-diffraction interferometer," (abstract only), *J. Opt. Soc. Am.* **62**(5), 737 (1972).
8. G. E. Sommargren, "Phase shifting diffraction interferometry for measuring extreme ultraviolet optics," in *OSA Trends in Optics and Photonics on Extreme Ultraviolet Lithography*, G. D. Kubiak and D. Kania, Eds., Vol. **4**, 108–112 (1996).
9. H. Kihm and S. W. Kim, "Oblique fiber optic diffraction interferometer for testing spherical mirrors," *Opt. Eng.* **44**(12), 125601-1~4 (2005).
10. G. E. Sommargren, "Diffraction methods raise interferometer accuracy," *Laser Focus World* **32**(8), 61–71 (1996).